

Cell shape recognition by colloidal cell imprints: Energy of the cell-imprint interactionJosef Borovička,¹ Simeon D. Stoyanov,^{2,3,4} and Vesselin N. Paunov^{1,*}¹*Department of Chemistry, The University of Hull, Hull HU6 7RX, United Kingdom*²*Laboratory of Physical Chemistry and Colloid Science, Wageningen University, 6703 HB Wageningen, Netherlands*³*Unilever R&D Vlaardingen, Olivier van Noortlaan 120, 3133 AT Vlaardingen, Netherlands*⁴*Department of Mechanical Engineering, University College London, Torrington Place, London WC1E 7JE, United Kingdom*

(Received 5 May 2015; published 30 September 2015)

The results presented in this study are aimed at the theoretical estimate of the interactions between a spherical microbial cell and the colloidal cell imprints in terms of the Derjaguin, Landau, Vervy, and Overbeek (DLVO) surface forces. We adapted the Derjaguin approximation to take into account the geometry factor in the colloidal interaction between a spherical target particle and a hemispherical shell at two different orientations with respect to each other. We took into account only classical DLVO surface forces, i.e., the van der Waals and the electric double layer forces, in the interaction of a spherical target cell and a hemispherical shell as a function of their size ratio, mutual orientation, distance between their surfaces, their respective surface potentials, and the ionic strength of the aqueous solution. We found that the calculated interaction energies are several orders higher when match and recognition between the target cell and the target cell imprint is achieved. Our analysis revealed that the recognition effect of the hemispherical shell towards the target microsphere comes from the greatly increased surface contact area when a full match of their size and shape is produced. When the interaction between the surfaces of the hemishell and the target cell is attractive, the recognition greatly amplifies the attraction and this increases the likelihood of them to bind strongly. However, if the surface interaction between the cell and the imprint is repulsive, the shape and size match makes this interaction even more repulsive and thus decreases the likelihood of binding. These results show that the surface chemistry of the target cells and their colloidal imprints is very important in controlling the outcome of the interaction, while the shape recognition only amplifies the interaction. In the case of nonmonotonous surface-to-surface interaction we discovered some interesting interplay between the effects of shape match and surface chemistry which is discussed in the paper. The results from this study establish the theoretical basis of cell shape recognition by colloidal cell imprints which, combined with cell killing strategies, could lead to an alternative class of cell shape selective antimicrobials, antiviral, and potentially anticancer therapies.

DOI: [10.1103/PhysRevE.92.032730](https://doi.org/10.1103/PhysRevE.92.032730)

PACS number(s): 87.17.Rt, 82.70.Dd, 41.20.Cv, 05.70.Ce

I. INTRODUCTION

Shape-specific recognition of microbial cells has recently been established as a new and growing field with numerous applications, including microbial detection [1,2] and extraction [3] as well as alternative types of colloidal antibodies [4]. Dickert and Hayden [1] used shape recognition of microbes to produce a bioanalytical tool based on patterned solid surfaces with polyurethane and a sol-gel process which imprint the surface of various genera of yeast. The incubation of different genera of yeast cells with such patterned surface led to their immobilization and the ability to distinguish between them [1]. A similar approach of immobilizing microbial organisms onto solid surfaces containing the sol-gel imprints was also employed by Cohen *et al.* [2] The same principle was used for extraction of bacterial spores on the surfaces of patterned microbeads [3]. “Key-lock” interactions have also been recently demonstrated by Sacanna *et al.* [5,6] in a colloidal system capable of programmed binding into composite clusters depending on the particle shape. Recently, we created colloidal particles which are partial imprints of microbial cells [4,7]. This was achieved by templating silica on the surface of the target cells followed by their fragmentation and subsequent cell removal by bleaching. After surface

treatment, the silica shells were able to selectively bind to the target cells in a mixture with other microbial cells of different shape [4,7].

Here we explore the theoretical basis of the shape and size recognition of the target cells by their matching colloid imprints. We develop a theoretical analysis which represents an extension of the Derjaguin, Landau, Vervy, and Overbeek (DLVO) theory [8,9] which considers the van der Waals and the electric double layer interactions, adapted for the geometry of a spherical target cell interacting with its hemispherical-shell replica. We will examine the role of various factors, including the respective orientation of the two interacting species, and their size ratio, along with the surface potentials of the spherical cell and the hemispherical shells and the ionic strength of the aqueous solution. There are many theoretical approaches which may be used to compute the colloidal interaction forces in such complex geometry via numerical methods; however, approximate analytical formulas are available only in the limiting cases of interactions, such as those between two infinite plates, between two spherical colloid particles, and between a sphere and an infinite plane [10–21].

The Derjaguin approximation, which involves the calculation of colloidal interactions via the summation of the interactions of infinitesimal surface elements of planar geometry, can be extended and generalized for objects of nonspherical shapes such as cylinders [8,22–24]. Bhattacharjee and

*Corresponding author: V.N.Paunov@hull.ac.uk

Elimenech have developed the surface element integration (SEI) technique—a similar method whereby the integration domain does not only cover the opposing faces of the interacting species but also the retrograde interface [25,26]. This technique has been employed, for instance, to estimate the interactions between spherical particles and cylindrical pores or spherical particles and rough surfaces [27,28]. However, for the purposes of our calculation this technique [25,26] although more accurate than the Derjaguin approximation, does not bring obvious theoretical advantage and allows only numerical estimation of the colloid interaction. Given that the typical cell size is a few micrometers (e.g., bacteria), the SEI method could not clearly reveal the physics of the interaction and the role of the cell-imprint geometrical factors. Here, we present an adaptation of the Derjaguin approximation for the estimation of the colloidal forces between a spherical target cell and a hemispherical shell which corresponds to the colloidal cell imprint of the target cell.

We stress that all calculations here are done here only for illustrative purposes which demonstrate qualitatively the effect of the mismatch of the radius of curvature of the inner surface of the hemispherical shell and the radius of curvature of the target cells. We also examine the interplay between the van der Waals forces and the electrostatic forces in the total interaction energy in this configuration. Here we derive simple and approximate analytical formulas for the interaction between target cells and matching hemispherical shells which enable us to clarify the role of the surface charge (potential) for the interaction between cells and their colloidal imprints. We also derive approximate analytical formulas for the interaction force and interaction energy between a hemispherical shell and a target microsphere (cell) at different mismatches of their size and orientation.

II. THEORETICAL BACKGROUND

Let us consider the interaction between a spherical cell of radius a_1 and a hemispherical shell of silica of thickness δ and inner radius of curvature a_2 . In order to explore the effect of surface forces on the hemispherical shell (hemishell)—particle recognition we assume that their surface potentials in aqueous solution can be different due to their different material properties and different ionizable groups on their surfaces. For the sake of completeness, we will examine the influence of the size ratio between the spherical cell and the hemispherical shell both in the case when shape recognition occurs, that is, when the cell faces the interior of the hemispherical shell, as well as when the recognition does not occur (see Fig. 1 for a scheme detailing the scenarios for which we have performed our calculations).

Here we aim to demonstrate how the energy of interaction between a hemispherical colloidal imprint and a spherical cell scales with the match in their size and orientation, which shows the magnitude of the effect of the cell shape recognition. As shown in our numerical analysis, the energy of attractive interaction can increase by two to three orders of magnitude upon cell shape match compared to a point contact which corresponds to interaction between a spherical cell and a spherical particle (or colloid imprint with unfavorable orientation with respect to the cell).

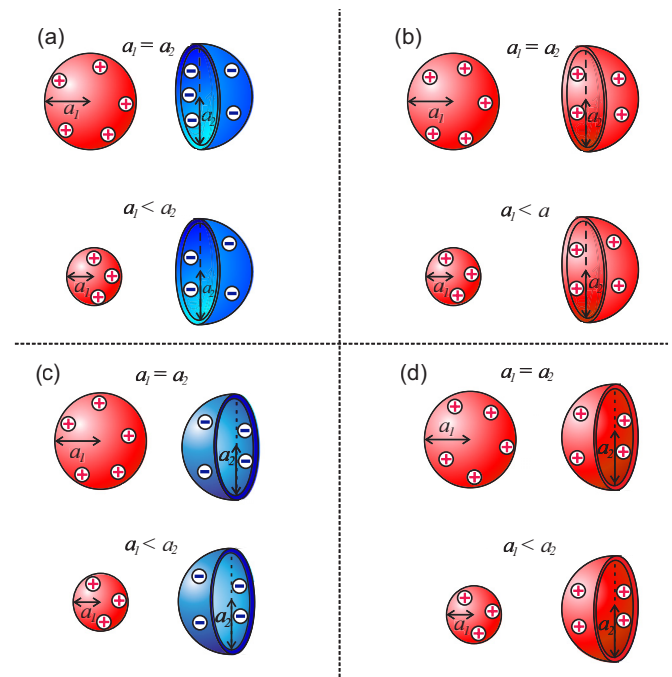


FIG. 1. (Color online) A scheme depicting the different scenarios of interactions between a hemispherical shell of inner radius a_2 and a spherical cell of radius a_1 . The red and blue colors signify positive and negative surface potentials, respectively. The scenario (a) involves the interaction of an oppositely charged sphere and its imprint arranged in a manner which leads to recognition; in (b) the surfaces geometrically match but have the same surface potential. Situations (c, d) depict analogous interactions of species which are geometrically or orientation mismatched; hence shape recognition does not occur.

A. Interaction energy between a spherical cell and the outer surface of a hemispherical shell

The interaction between a spherical cell and the outer part of its silica hemispherical shell imprint was calculated in a similar way as the interaction between two spherical colloid particles, as follows. The nonretarded van der Waals interaction energy E_{VW} between two semi-infinite phases is [29]

$$E_{VW}(h) = -\frac{A_H}{12\pi h^2}, \quad (1)$$

where h is their separation. Here A_H is the compound Hamaker constant for the case of two semi-infinite phases interacting across an aqueous film of thickness h . Obviously, this is strictly correct only in the case of two uniform spherical particles. In the case of a hemispherical shell, oppositely orientated towards a spherical cell, the formula will be similar but with a different effective value of the Hamaker constant, taking into account the fact that the shell is hollow and there is an aqueous phase on the other side of the shell. However, the functional dependence of the van der Waals energy of interaction from the film thickness, h , will be the same. Using the Derjaguin approximation one can obtain the following expression for the van der Waals interaction energy [26]:

$$U_{VW} = -\frac{A_H a_1 a_2}{6(a_1 + a_2)D}, \quad (2)$$

where D is the distance of closest approach between the two surfaces. When $a_1 = a_2 = a$, then

$$U_{VW} = -\frac{A_H a}{12D}. \quad (3)$$

The sphere-sphere electric double layer interaction energy can be estimated by using the linear superposition expression for the interaction between two flat surfaces (per unit area) [30]:

$$E_{EL}(h) = B \exp(-\kappa h), \quad B = 32\varepsilon_0\varepsilon_r\kappa\gamma_1\gamma_2\left(\frac{kT}{ve}\right)^2, \quad (4)$$

where ε_0 is the permittivity of vacuum, ε_r is the relative dielectric permittivity, and κ is the inverse Debye screening length. $\gamma_i = \tanh(\varphi_i/4)$ and $\varphi_i = ve\psi_i/kT$ ($i = 1, 2$) where k is the Boltzmann's constant, v is the valency of the electrolyte, e is the electronic charge, T is the absolute temperature, and ψ_i are surface electric potentials for the target and the imprint surfaces. The total free energy of interaction between plane-parallel surfaces, according to the DLVO theory, is a sum of the van der Waals and electrostatic contributions:

$$E(h) = E_{VW}(h) + E_{EL}(h). \quad (5)$$

By applying the Derjaguin method [8,9] to Eq. (4) one obtains the electrostatic energy of interaction in this geometric configuration [1]:

$$U_{EL} = 2\pi B \left(\frac{a_1 a_2}{a_1 + a_2} \right) \frac{1}{\kappa} \exp(-\kappa D). \quad (6)$$

When the cell and the hemispherical shell (inner radius) are equally sized, $a_1 = a_2 = a$, then

$$U_{EL} = \frac{\pi a B}{\kappa} \exp(-\kappa D). \quad (7)$$

The total interaction energy U_{TOTAL} was then calculated by summing Eqs. (2) and (6):

$$U_{TOTAL} = U_{VW} + U_{EL}, \quad (8)$$

$$U_{total} = -\frac{A_H a_1 a_2}{6(a_1 + a_2)D} + 2\pi B \left(\frac{a_1 a_2}{a_1 + a_2} \right) \frac{1}{\kappa} e^{-\kappa D}, \quad (9)$$

which for equal curvatures reduces to

$$U_{TOTAL} = -\frac{A_H a}{12D} + \frac{\pi B a}{\kappa} e^{-\kappa D}. \quad (10)$$

Please note that Eqs. (9) and (10) are approximate and are valid only within the framework of the Derjaguin approximation [8] in colloid science for the DLVO interaction between two spherical particles in an aqueous solution, which requires that the radius of action of the colloid forces between the particle surfaces is much smaller than the radius of curvature a of the particle surfaces. Geometrically, this situation corresponds to Figs. 1(c) and 1(d) in our diagram of interaction between a spherical cell and oppositely (unfavorably) orientated hemispherical shell.

B. Interaction energy between a spherical cell and the inner surface of a hemispherical shell

We have adapted the Derjaguin method to our specific scenario of the interaction of a spherical cell and the inner part of the hollow hemispherical shell, corresponding to Figs. 1(a) and 1(b). First we consider the case where the hemispherical shell has larger or equal radius of curvature than the spherical cell, $a_1 \leq a_2$. The complementary case of a hemispherical shell with smaller radius of curvature than the spherical cell ($a_1 \geq a_2$) is considered in the following subsection.

1. Interaction between a target spherical cell and a larger hemispherical shell

Let us consider the interaction between a spherical cell of radius a_1 and a hemispherical shell of radius a_2 , where $a_1 \leq a_2$. The schematic diagram of this case is presented in Fig. 2(a). The surface of the spherical particle and the inner surface of the hemispherical shell can be described by the following equations:

$$z_1(r) = a_1^2 \sqrt{1 - \frac{r^2}{a_1^2}}, \quad z_2(r) = a_2^2 \sqrt{1 - \frac{r^2}{a_2^2}}. \quad (11)$$

The running distance $H_S(r)$ between the two surfaces is

$$H_S(r) = D + a_1 - a_2 - z_1(r) + z_2(r). \quad (12)$$

For a small degree of mismatch between the hemispherical shell and the target cell and a small radius of action of the surface forces compared to both a_1 and a_2 we can use the Derjaguin approach to expand Eq. (12) in series:

$$H_S(r) = D + \frac{1}{2} \left(\frac{1}{a_1} - \frac{1}{a_2} \right) r^2 + O(r^4). \quad (13)$$

The latter is equivalent to approximating the spherical parts of both surfaces with paraboloid surfaces with the same radius of curvature. If $E(h)$ is the free surface energy of interaction of

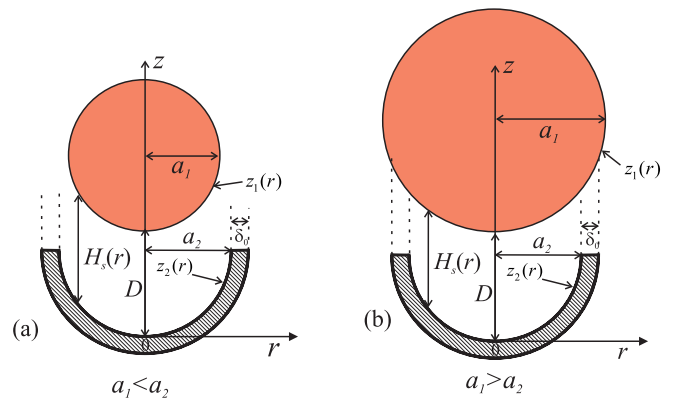


FIG. 2. (Color online) Schematics of the interaction between a spherical cell of radius a_1 and a hemispherical shell of inner radius of curvature a_2 at a distance D between their surfaces. (a) The cell radius of curvature is smaller than (or equal to) the inner radius of curvature of the hemispherical shell. (b) The cell radius of curvature is larger than the inner radius of curvature of the hemispherical shell. In this case the rim of the hemispherical shell (of thickness δ) also contributes to the interaction.

two plane-parallel surfaces of the same properties as the target cell and the hemishell, then the Derjaguin approximation in this case should be written as follows:

$$U = \iint_A E[H_S(r)] dx dy = \int_0^{2\pi} d\varphi \int_0^{a_1} dr [r E[H_S(r)]]. \quad (14)$$

Here we have changed the Cartesian coordinates (x, y) to polar coordinates (r, φ) , according to the transformation

$$x = r \cos \varphi, \quad y = r \sin \varphi, \quad r^2 = x^2 + y^2. \quad (15)$$

Note that due to this approximation the surface integration of the interaction energy cannot be done from $r = 0$ to $r = \infty$ as in the original work of Derjaguin for two spheres as this would give a divergence due to the infinite parabolic surfaces. The integration of the surface elements of these two surfaces will be done in an approximate manner only up to the smaller radius of curvature, i.e., up to the radius of curvature of the particle in the case depicted in Fig. 2(a). This is justified as we are mostly interested in target cells which are at least two orders of magnitude larger than the Debye length and the perimeter of action of the van der Waals interactions. Hence the integration in Eq. (14) can be done in a general form as follows:

$$U = 2\pi \int_D^{H_1} E[h(r)] d\left(\frac{r^2}{2}\right) \approx \frac{2\pi a_1 a_2}{a_2 - a_1} \int_D^{H_1} E(h) dh. \quad (16)$$

Here $H_1 = H_S(r = a_1)$ for this particular case [Fig. 2(a)]. Using Eqs. (1) and (16) for the van der Waals interaction energy in this configuration we obtain

$$U_{VW} = -\frac{a_1 a_2 A_H}{6(a_2 - a_1)} \left[\frac{1}{D} - \frac{2a_2}{(2Da_2 + a_1 a_2 - a_1^2)} \right]. \quad (17)$$

$$U_{EL} = \frac{2\pi B a_1 a_2}{\kappa(a_2 - a_1)} \left[e^{-\kappa D} - e^{-\frac{\kappa(2Da_2 + a_1 a_2 - a_1^2)}{a_2}} \right]. \quad (18)$$

The total interaction energy is a sum of Eqs. (17) and (18), $U_{TOTAL} = U_{VW} + U_{EL}$. Please note that although there is the term $(a_2 - a_1)$ in the denominators of both Eqs. (17) and (18), they do not diverge at $a_1 = a_2$ which corresponds to equal (matching) radii of curvature. Thus for matching spherical target cell and hemispherical shell ($a_1 \rightarrow a$, $a_2 \rightarrow a$), the modified Derjaguin approximations give

$$U_{VW} = -\frac{a^2 A_H}{12D^2}, \quad (19)$$

$$U_{EL} = \pi a^2 B e^{-\kappa D}, \quad (20)$$

$$U_{TOTAL} = -\frac{a^2 A_H}{12D^2} + \pi a^2 B e^{-\kappa D}. \quad (21)$$

One can see that there is a profound difference between this formula, Eq. (21), and the case of interaction of two spherical particles of equal radius, Eq. (10), when it comes to the dependence on the distance between the particle surfaces and the particle radius. Since the latter case is also similar to the case of a misoriented hemishell and a spherical cell, the difference between Eqs. (21) and (10) gives the difference between the interaction energies in the case of the favorable and unfavorable orientations of the hemispherical shell with respect to the matching target cell. These results call for some further analysis. The ratio of the van der Waals interaction

energies for the case of favorable (recognition), Eq. (19), and unfavorable orientation, Eq. (3), gives

$$\frac{U_{VW}^{\text{favorable}}}{U_{VW}^{\text{unfavorable}}} = \frac{-\frac{a^2 A_H}{12D^2}}{-\frac{A_H a}{12D}} = \frac{a}{D} \gg 1. \quad (22)$$

Here it is assumed that the Hamaker constant, A_H , is similar in both cases which may be justified for hemishell thickness larger than several tens of nanometers. This means that for a large enough hemispherical shell in unfavorable orientation [Figs. 1(c) and 1(d)], it will interact with the target spherical cell similarly to a spherical silica particle. Similarly, for thick enough silica hemispherical shells in a favorable orientation [Figs. 1(a) and 1(b)], the Hamaker constant will have a very similar value which justifies the comparison in Eq. (22). Note that since $D \ll a$, the van der Waals interaction upon target recognition (in favorable orientation) is much stronger than those in unfavorable orientation where there is no recognition. Similarly, the comparison of the electrostatic interaction energies, Eqs. (20) and (7), gives

$$\frac{U_{EL}^{\text{favorable}}}{U_{EL}^{\text{unfavorable}}} = \frac{\pi a^2 B \exp(-\kappa D)}{\frac{\pi a B}{\kappa} \exp(-\kappa D)} = \kappa a \gg 1. \quad (23)$$

For typical values of $a = 3 \mu\text{m}$ for bacterial cells and salt concentration $0.1 M$, $\kappa^{-1} \approx 3 \text{ nm}$ which gives $\kappa a = 1000$. This corresponds to an electrostatic interaction energy upon recognition [Figs. 1(a) and 1(b)] of the target cell by the hemispherical shell, three orders of magnitude larger compared to the same interaction in an unfavorable orientation [no recognition, Figs. 1(c) and 1(d)]. This means that if the electrostatic interaction is attractive (e.g., for oppositely charged target particle and hemishell), the size-based recognition between the target cell and the hemishell would amplify the interaction, making their attraction much stronger. However, if the electrostatic interaction is repulsive (e.g., for like charged target cell and hemispherical shell) the favorable orientation will make it even more repulsive.

2. Interaction between a target spherical cell and a smaller hemispherical shell

Let us consider the complementary case where the hemispherical shell has a smaller inner radius than the radius of the target spherical cell, $a_1 \geq a_2$, as presented in Fig. 2(b). In this case, we can also derive approximate formulas for the interaction energy using the Derjaguin approach, but the integration of the interacting surface elements between the two surfaces has two contributions:

$$U = U_S + U_R, \quad (24)$$

where

$$U_S = \iint_{A_S} E(H_S(r)) dx dy = \int_0^{2\pi} d\varphi \int_0^{a_2} dr \{r E[H_S(r)]\} \quad (25)$$

is the interaction between the inner surface A_S of the hemispherical shell and its vertical projection over the target cell surface. Here the upper boundary of the surface integral ends at $r = a_2$ instead of $r = a_1$ in the case sketched in Fig. 2(a).

In addition to this contribution, there is also a contribution from the rim of the hemispherical shell interacting with its projection onto the target cell's surface,

$$U_R = \iint_{A_R} E[H_S(r)] dx dy = \int_0^{2\pi} d\varphi \int_{a_2}^{a_2+\delta} dr \{r E[H_S(r)]\}. \quad (26)$$

Here A_R is the projection of the rim surface onto the target cell surface. In Eqs. (25) and (26), $H_S(r)$ is the running distance between the two surfaces, defined by Eq. (12). The parameter δ in Eq. (26) is defined as follows:

$$\delta = \begin{cases} \delta_0, & a_1 - a_2 \geq \delta_0 \\ a_1 - a_2, & a_1 - a_2 < \delta_0 \end{cases}. \quad (27)$$

By using the same level of approximation of the two interacting surfaces with paraboloids as in Eq. (13) and carrying out the integration in Eq. (25) we obtain

$$U_S \approx \frac{2\pi a_1 a_2}{a_2 - a_1} \int_D^{H_2} E(h) dh, \quad (28)$$

where $H_2 = H_S(a_2)$. Using Eq. (12) one can expand the integral in Eq. (26) in series for small values of the parameter $\delta/a_2 \ll 1$ to obtain

$$U_R = 2\pi \delta a_2 E(H_2) + O(\delta^2). \quad (29)$$

Equation (29) can be obtained in an approximate manner by simply multiplying the surface free energy, $E(H_2)$, by the approximate area of the hemispherical shell rim, $2\pi a_2 \delta$. Note that Eq. (29) is valid only when $\delta \ll a_2$. Substituting Eqs. (1), (4), and (5) into Eq. (28) and carrying out the integration gives

$$U_S \approx \frac{2\pi a_1 a_2}{a_2 - a_1} \left[\frac{B}{\kappa} (e^{-\kappa D} - e^{-\kappa H_2}) + \frac{A_H}{12\pi} \left(\frac{1}{H_2} - \frac{1}{D} \right) \right]. \quad (30)$$

Note that U_S in Eq. (30) is not divergent when $a_1 \rightarrow a_2$. Similarly, the combination of Eqs. (1), (4), and (5) with Eq. (29) gives

$$U_R \approx 2\pi a_2 \delta \left[B e^{-\kappa H_2} - \frac{A_H}{12\pi H_2^2} \right], \quad a_1 > a_2. \quad (31)$$

The total interaction energy in this case is given by Eq. (24) where $H_2 = H_S(a_2)$ is calculated from Eq. (13). Note that when the inner radius of the hemispherical shell gets very close to that of the target cell, $a_1 = a_2 = a$, Eq. (30) can be expanded in power series for small values of $(a_2 - a_1)$ to give

$$U_S \approx -\frac{a^2 A_H}{12D^2} + \pi a^2 B e^{-\kappa D}, \quad (a_1 = a_2 = a). \quad (32)$$

The last equation coincides with Eq. (21) which shows that the matching sizes of the hemishell and the target spherical cell give the same asymptotic results for the interaction energy. In this case, however, $U_R = 0$, by definition as the area A_R of the projection of the rim onto the target cell surface, is zero for the matching hemispherical shell and target spherical cell.

The comparison between the contributions of the inner shell surface, Eq. (30), and the rim, Eq. (31), shows that their ratio is proportional to δ/a_2 , where for typical values of δ and a_2 , $\delta/a_2 \ll 1$. Hence the contribution of the hemishell rim to the interaction with the target cell can be neglected within the scope and accuracy of this model.

III. RESULTS AND DISCUSSION

Here, we estimated numerically only the interaction between target cells of radius smaller or equal to those of the hemispherical shell. Our aim here is to capture the physics of the recognition between a colloid imprint and a matching cell of spherical geometry. We used Eqs. (8)–(10); (17) and (18); (24); and (30) and (31) to model the interaction of the target spherical cells with hemispherical shells. For the sake of numerical estimates, we use target spherical cells and the hemispherical shells (colloid imprints) are made of silica. The Hamaker constants of the cells and silica A_{ii} of 1.15×10^{-19} J and 5×10^{-19} J, respectively [2], result in the effective Hamaker constant A_H in an aqueous medium ($A_{ii} = 4.85 \times 10^{-20}$ J) of 5.79×10^{-20} J. We examined the energy of interaction for the following ionic strengths of the aqueous medium, $I = 1 \times 10^{-2}$ M, $I = 5 \times 10^{-3}$ M, and $I = 1 \times 10^{-5}$ M.

The calculations were done at several different values of the surface potentials ($\psi_s = \pm 25$ mV, ± 35 mV, and ± 45 mV) of the hemishells and the target cells. We explored the influence of the ionic strength of the aqueous medium in which the target particles are incubated with the hemishells, and the role of their surface potentials and the separation between them, as well as the size ratio and the orientation of the hemishell and the target cell. The influence of the separation was studied on a $1\text{-}\mu\text{m}$ cell and a matching silica hemispherical shell replica over separations of 5–100 nm.

We set the surface-to-surface separation larger than 5 nm as the silica imprints have certain surface roughness and also may be coated with polyelectrolytes as the ones in Ref. [4]. The influence of the size ratio was studied at constant separation of 10 nm and constant diameter of the silica hemishell $a_1 = 1 \mu\text{m}$ while varying the diameter of the spherical target cell for a_1/a_2 ratios from 0.05 to 1. The orientation factor was probed by assuming the target spherical cell faced either the interior of the hemishell [as in Figs. 1(a) and 1(b)] or its outer, convex, spherical side [as in Figs. 1(c) and 1(d)].

We found that the recognition between oppositely charged interacting species energetically favors the binding of the target cell to the inner surface of the matching silica hemishell imprint in comparison to the scenario where the binding occurs on the outer part of the hemispherical shell surface. Considering the scenario where the separation D was varied, it has been noted that the U_{VW} between the inner part of the silica hemishell and the target cell was about $-4.8 \times 10^4 kT$ at the distance of 5 nm and becomes much weaker when D is 100 nm; then the interaction energy is approximately $119kT$. At these values of the parameters, the van der Waals interaction energy, U_{VW} between a cell facing the convex side of its matching silica hemishell is $-238kT$ when they are separated by 5 nm and about $12kT$ when their separation reaches 100 nm. This shows us that the matching geometry increases the van der Waals attraction approximately tenfold in the case of the relatively long distance interactions and about 200-fold in the case of 5 nm separation. This explains the importance of the size recognition between the target cell and the matching hemishell. Furthermore, the interaction energy between the cell and the silica hemishell oriented so that they match their hemishell is of the order of $10^4 - 10^5 kT$ while the interaction energy between the mismatches is on the order of hundreds of kT .

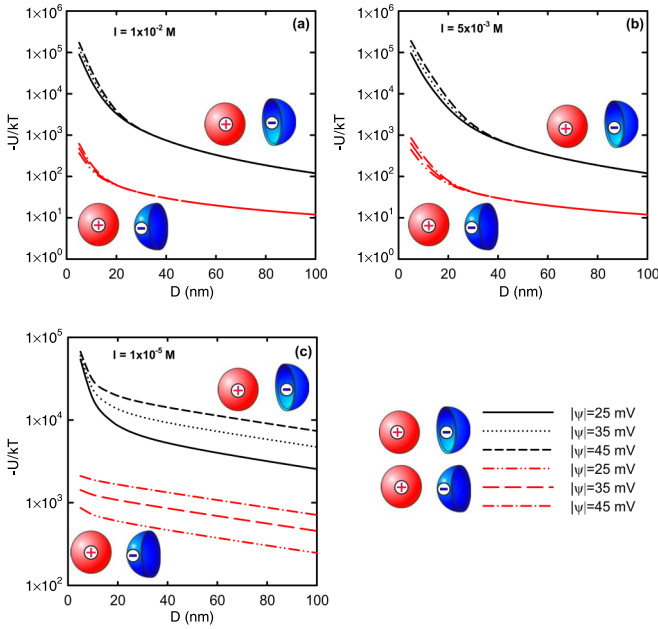


FIG. 3. (Color online) Total interaction energy between the spherical target cell of radius $a_1 = 1 \mu\text{m}$ and its matching silica hemispherical cell imprint ($a_2 = 1 \mu\text{m}$) as a function of distance at various ionic strengths: (a) $I = 1 \times 10^{-2} M$, (b) $I = 5 \times 10^{-3} M$, and (c) $I = 1 \times 10^{-5} M$. The different curves correspond to different surface potentials and orientations of the hemispherical and the target spherical cell.

The screening effect which arises from the salt ions present in the medium has a pronounced effect in both geometries. The electrostatic contribution to the total interaction energy generally increases for all three values of the ionic strength of the medium in the case of the mismatch situations. It can also be seen that a larger increase of the electrostatic interactions contribution occurs at about $D = 20$ nm (see Fig. 3).

The results presented in Fig. 4 show that at the relatively low ionic strength of the aqueous medium, $I = 1 \times 10^{-5} M$, which corresponds to $\kappa^{-1} = 100$ nm, the electric double layer interactions, U_{EL} , weaken and at distances D smaller than 10 nm the attractive van der Waals interaction energy, U_{VW} , becomes dominant even when the target cell and the hemispherical imprint carry the same surface potential. The size matching between the target cell and the silica hemispherical shell has also proven to be very important. Figure 5 demonstrates that when oppositely charged species are separated by 10 nm the difference between the U_{TOTAL} when $a_1/a_2 = 0.05$ and $a_1/a_2 = 1$ is about three orders of magnitude and that there is a difference of two orders of magnitude in the interaction energy for orientation where the hemispherical imprint faces the cell via its concave side compared with the case when it faces the cell via its convex part.

The analysis performed here with DLVO forces shows that if the net surface force is attractive, the cell shape match, $a_1 = a_2 = a$, leads to a huge amplification of the overall attraction energy which results in recognition and binding of the cell by the imprint. If the interaction is repulsive, the shape match would amplify the repulsion and no cell recognition and binding will occur. Similar situations can

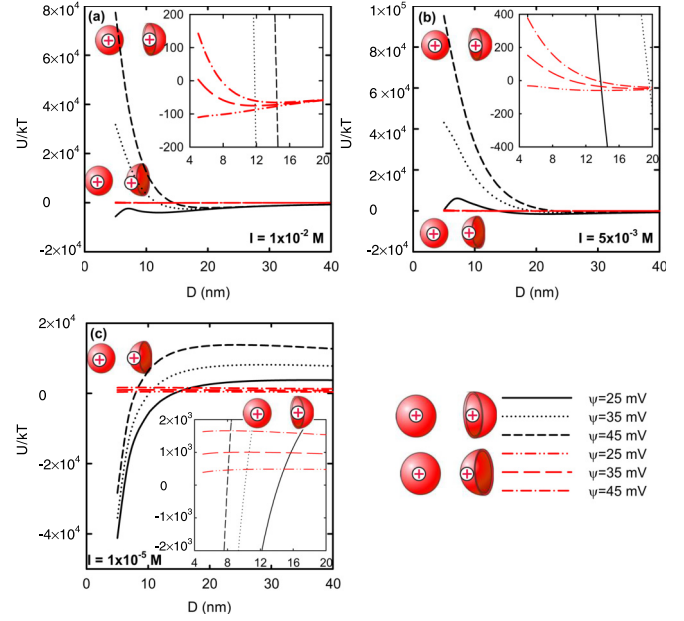


FIG. 4. (Color online) Total interaction energy between the target cell and its hemispherical imprint as a function of distance at various levels of ionic strength, I , and equal surface potentials ψ (see legend). (a) $I = 1 \times 10^{-2} M$, (b) $I = 5 \times 10^{-3} M$, and (c) $I = 1 \times 10^{-5} M$. The figure insets illustrate the variation of the interaction energy with the surface-surface distance for the unfavorable cell-imprint orientation. Note that the interaction energy vs distance curve in the unfavorable cell-imprint orientation only looks flat on a scale of variation of the interaction energy with the distance, which is much larger by magnitude.

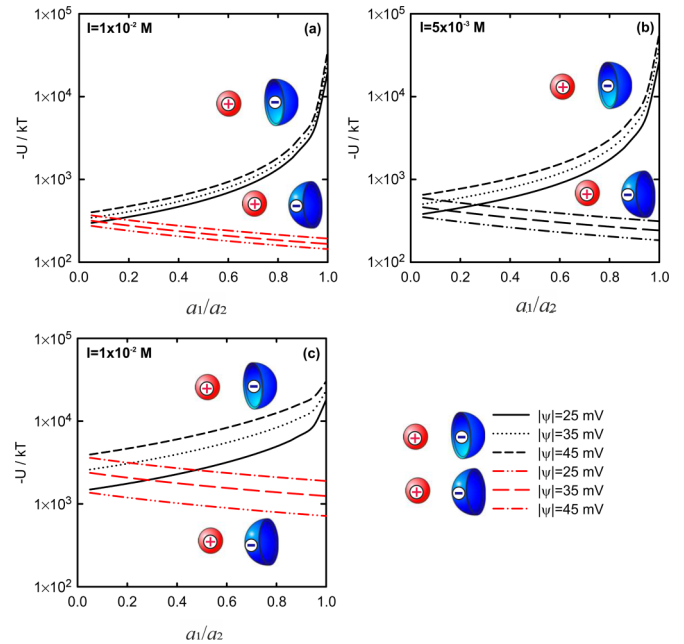


FIG. 5. (Color online) Total interaction energy between the target microsphere of radius $a_1 = 1 \mu\text{m}$ and its silica hemispherical imprint as a function of a_1/a_2 ratio at various ionic strengths, I , and surface potentials ψ . The target particle and the hemispherical imprint are oppositely charged. (a) $I = 1 \times 10^{-2} M$, (b) $I = 5 \times 10^{-3} M$, and (c) $I = 1 \times 10^{-5} M$. Here the separation is fixed to $D = 10$ nm.

occur for nonmonotonic surface-surface interaction potential with a minimum but the binding of the cell to the imprint would not happen at contact and the overall binding energy would be smaller. For example, for imprints coated with a specific protein antibody, their radius of action is limited to a few nm distance from the cell wall which compared to the cell size ($1 - 5 \mu\text{m}$) is more likely to result in binding when there is minimal size mismatch between a cell and its surface functionalized cell imprint. This analysis is outside of the scope of the present work and will be a subject of further detailed studies.

In addition to the DLVO surface forces which are fairly universal and exist between the cells and their imprints in biological scenarios, one may also consider other non-DLVO forces depending on the specific coating on the imprint surface. For example, incorporation of short-ranged hydration repulsion interactions due to adsorbed layer of highly hydrated counterions [7] can be done similarly to Eq. (4),

$$E_{\text{hydration}}(h) = f_0 \exp(-h/\lambda_0), \quad (33)$$

with typical values $f_0 = 3 - 30 \text{ mJ m}^{-2}$ and $\lambda_0 = 1.1 \text{ nm}$ for 1:1 electrolyte. The application of the Derjaguin's approach for the case of hemispherical imprint and a spherical cell would give the following equivalent of Eq. (18):

$$U_{\text{hydration}}(D) = \frac{2\pi f_0 \lambda_0 a_1 a_2}{(a_2 - a_1)} \left[e^{-\frac{D}{\lambda_0}} - e^{-\frac{(2Da_2 + a_1 a_2 - a_1^2)}{\lambda_0 a_2}} \right]. \quad (34)$$

Hydrophobic attraction [31] could also be introduced in a straightforward manner, as in Eq. (4):

$$E_{\text{hydrophobic}}(h) = -2\gamma_1 \exp(-h/\lambda_1), \quad (35)$$

with typical values of $f_0 = 3 - 30 \text{ mJ m}^{-2}$ and $\lambda_1 = 12 - 15 \text{ nm}$ for hydrophobized surfaces. This interaction potential would give the following equivalent of Eq. (18):

$$U_{\text{hydrophobic}}(D) = -\frac{4\pi \gamma_1 \lambda_1 a_1 a_2}{(a_2 - a_1)} \left[e^{-\frac{D}{\lambda_1}} - e^{-\frac{(2Da_2 + a_1 a_2 - a_1^2)}{\lambda_1 a_2}} \right]. \quad (36)$$

Incorporation of the adhesion promoted by coatings of immobilized protein antibodies or polymer adsorption layers on the colloid imprint is more complicated and requires much more specific information about the surface-surface interaction potential with the cell surface. This will be part of a future modeling study and publications.

IV. CONCLUSIONS

We have adapted the Derjaguin approach to derive analytical formulas for the energy of interaction between a target

spherical cell and a colloid imprint of hemispherical geometry. The findings from this modeling clearly demonstrate that the size match between the target cell and the hemispherical shells which represent the cell-colloid imprint interaction have a more rigorous theoretical basis. We have fixed the target cell shape to be spherical and only explored the role of the size mismatch and the cell material parameters such as surface potentials and Hamaker constant as well as the ionic strength of the medium. We have demonstrated that the energy of interaction between the hemispherical shell and the target cell is several orders of magnitude higher when the size recognition between them is achieved. We find that when the hemispherical shell and the target cell are equally sized, the energy of interaction is larger in the case of favorable orientation of the cell towards the interior of the hemispherical shell replica. The latter is stronger by the factor of a/D in the case of the van der Waals interactions compared to the unfavorable orientation when the cell approaches the outer part of the hemispherical shell. In the case of electrostatic interactions, upon favorable approach of the cell towards the inner side of the hemispherical shell we estimated levels of interaction energy which are κa times stronger in comparison to the unfavorable orientation.

Generally, the size recognition of the spherical target cell and its hemispherical colloid imprint amplifies the magnitude of the interaction energy between their surfaces. If the interaction energy between the target cell and the hemispherical shell is attractive, the size match amplifies the attraction. If the interaction is repulsive, the size and shape recognition amplifies the repulsion. For micrometer sized target cells and moderate ionic strength this can result in more than three orders of magnitude difference in the interaction energy. Furthermore, we have shown a very strong effect on the interaction by the size mismatch between the target cell and the hemispherical shell in both situations of favorable and unfavorable orientation. Since the interaction energy between the colloidal imprint and its target cell is linked to their binding constant through an exponential dependence, even moderate increase of the energy of attraction leads to an exponential increase of their binding constant. This justifies the approach of using colloidal cell-imprint particles which can bind strongly to their target cells based on their shape and size recognition.

ACKNOWLEDGMENTS

This work was supported by a BBSRC Industrial CASE studentship (Grant No. BB/F01807X/1) and Unilever R&D Vlaardingen (The Netherlands). The authors also appreciate financial support from EU COST action CM1101.

-
- [1] F. L. Dickert and O. Hayden, *Anal. Chem.* **74**, 1302 (2002).
- [2] T. Cohen, J. Starosvetsky, U. Cheruti, and R. Armon, *Int. J. Mol. Sci.* **11**, 1236 (2010).
- [3] S. Harvey, G. Mong, R. Ozanich, J. McLean, S. Goodwin, N. Valentine, and J. Fredrickson, *Anal. Bioanal. Chem.* **386**, 211 (2006).
- [4] J. Borovička, M. J. Metheringham, L. A. Madden, C. D. Walton, S. D. Stoyanov, and V. N. Paunov, *J. Am. Chem. Soc.* **135**, 5282 (2013).
- [5] S. Sacanna, W. T. M. Irvine, P. M. Chaikin, and D. J. Pine, *Nature* **464**, 575 (2010).
- [6] S. Sacanna, W. T. M. Irvine, L. Rossi, and D. J. Pine, *Soft Matter* **7**, 1631 (2011).
- [7] J. Borovička, S. D. Stoyanov, and V. N. Paunov, *Nanoscale* **5**, 8560 (2013).
- [8] B. V. Derjaguin and L. Landau, *Acta Physicochimica (URSS)* **14**, 633 (1941).
- [9] E. J. W. Verwey and J. T. G. Overbeek, *Theory of the Stability of Lyophobic Colloids* (Dover Publications, New York, 1999).

- [10] S. L. Carnie, D. Y. C. Chan, and J. Stankovich, *J. Colloid Interface Sci.* **165**, 116 (1994).
- [11] B. K. C. Chan and D. Y. C. Chan, *J. Colloid Interface Sci.* **92**, 281 (1983).
- [12] O. F. Devereux and P. L. D. Bruyn, *Interaction of Plane-Parallel Double Layers* (M. I. T. Press, Cambridge, MA, (1963).
- [13] A. B. Glendinning and W. B. Russel, *J. Colloid Interface Sci.* **93**, 95 (1983).
- [14] M. L. Grant and D. A. Saville, *J. Colloid Interface Sci.* **171**, 35 (1995).
- [15] N. E. Hoskin, *Philos. Trans. R. Soc. London A* **248**, 433 (1956).
- [16] N. E. Hoskin and S. Levine, *Philos. Trans. R. Soc., A* **248**, 449 (1956).
- [17] L. N. McCartney and S. Levine, *J. Colloid Interface Sci.* **30**, 345 (1969).
- [18] D. McCormack, S. L. Carnie, and D. Y. C. Chan, *J. Colloid Interface Sci.* **169**, 177 (1995).
- [19] H. Ohshima, T. W. Healy, and L. R. White, *J. Colloid Interface Sci.* **90**, 17 (1982).
- [20] H. Ohshima and T. Kondo, *J. Colloid Interface Sci.* **126**, 382 (1988).
- [21] J. Stankovich and S. L. Carnie, *Langmuir* **12**, 1453 (1996).
- [22] B. V. Derjaguin, in *Surface Forces*, edited by B. V. Derjaguin, V. Churaev, and V. M. Muller, translated from the Russian by V. I. Kisin, translation edited by J. A. Kitchener (Consultants Bureau, New York, 1987).
- [23] Z. Adamczyk, P. Belouschek, and D. Lorenz, *Ber. Bunsen-Ges. Phys. Chem.* **95**, 566 (1991).
- [24] L. R. White, *J. Colloid Interface Sci.* **95**, 286 (1983).
- [25] S. Bhattacharjee and M. Elimelech, *J. Colloid Interface Sci.* **193**, 273 (1997).
- [26] S. Bhattacharjee, M. Elimelech, and M. Borkovec, *Croat. Chem. Acta* **71**, 883 (1998).
- [27] S. Bhattacharjee and A. Sharma, *J. Colloid Interface Sci.* **187**, 83 (1997).
- [28] X. Huang, S. Bhattacharjee, and E. M. V. Hoek, *Langmuir* **26**, 2528 (2010).
- [29] H. C. Hamaker, *Physica* **4**, 1058 (1937).
- [30] G. John, *J. Colloid Interface Sci.* **51**, 44 (1975).
- [31] J. N. Israelachvili, *Intermolecular and Surface Forces*, 3rd ed. (Academic Press, Burlington, MA, 2011), pp. 361, 370.